

COMPTON J. TUCKER  
BRENT N. HOLBEN  
NASA/Goddard Space Flight Center  
Greenbelt, MD 20771  
JAMES H. ELGIN, JR.  
JAMES E. McMURTREY III  
Plant Genetics and Germplasm Institute  
Beltsville, MD 20705

# Relationship of Spectral Data to Grain Yield Variation

Significant linear relationships were found between various combinations of the red and photographic infrared radiance data collected and the grain yield within a winter wheat field.

## BACKGROUND

SEVERAL APPROACHES for remote sensing of winter wheat yield have been proposed. The Large Area Crop Inventory Experiment (LACIE) involving NASA, NOAA, and the USDA, was perhaps the most visible and the best known of various winter wheat yield prediction approaches. Simulation or regression models were used to predict wheat yield based upon climatic conditions (MacDonald and Hall, 1977).

Idso *et al.* (1977a,b) have proposed a method of winter wheat yield prediction using the stress degree day concept. That is, the final yield of a crop was hypothesized to be linearly related to the accumulated stress degree days over some critical period. This technique was developed in Phoenix, Arizona under irrigated conditions and is currently being evaluated in dryland winter wheat growing areas.

Hammond (1975) and Morain and Williams (1975) have discussed monitoring

---

**ABSTRACT:** *Two-band hand-held radiometer data from a winter wheat field, collected on 21 dates during the spring growing season, were correlated with within-field final grain yield. Significant linear relationships were found between various combinations of the red and photographic infrared radiance data collected and the grain yield. The spectral data explained ~64 percent of the within-field grain yield variation. This variation in grain yield could not be explained using meteorological data as these were similar for all areas of the wheat field. Most importantly, data collected early in the spring were highly correlated with grain yield, a five-week time window existed from stem elongation through anthesis in which the spectral data were most highly correlated with grain yield, and manifestations of wheat canopy water stress were readily apparent in the spectral data.*

---

The EarthSat Corp. (1976) has proposed a spring wheat yield prediction method. This approach differs from the LACIE approach in that NOAA meteorological satellite data were used to estimate grid cell precipitation which in turn drove the yield determination. Critical variables for this approach were the calculation of soil moisture and grid cell weather from the meteorological satellite data and the determination of crop phenology (LACIE, 1978).

wheat production with satellite remotely sensed data. Harlan and Liu (1975) and Colwell *et al.* (1977) have evaluated the use of Landsat data for inferring direct winter wheat grain yield predictions. Spectral data were used to estimate yield related variables such as stand density or leaf area index (LAI). Because grain yield is usually highly correlated to stand density or leaf area index, a direct estimate of final grain yield was usually possible (Colwell *et al.*, 1977). Colwell *et al.*

(1977) concluded that Landsat (i.e., spectral) data explained a considerable amount of yield variation which was not explained by meteorological data. In addition, Landsat derived yield predictions were as highly correlated with individual field yields as were estimates made using traditional sampling techniques, even, in some cases, if the Landsat data were collected several weeks before the field samples.

Heilman *et al.* (1977) reported a technique for estimating winter wheat grain yields using Landsat derived estimates of leaf area index coupled with an evapotranspiration model. More recently, Wiegand *et al.* (1979) discussed leaf area index estimates for winter wheat made from Landsat data and the implications for evapotranspiration and crop simulation modeling using these data.

Accurate inputs for crop canopy leaf area index are a necessity for successful evapotranspiration and crop simulation modeling. To achieve accurate leaf area index estimates from Landsat data, "ground-truth" sampling must occur which adequately samples the variability of the actual field leaf area index for enough Landsat pixels (~0.45 ha) to satisfy basic sampling theory requirements. This has often proven difficult to achieve. Heilman *et al.* (1977), Kanemasu *et al.* (1977), and Wiegand *et al.* (1979) all used three ground samples of 91 cm by 2 row widths (~30 cm) to establish each field's (>40 ha) leaf area index. Thus ~1 m<sup>2</sup> was used to determine the leaf area index of a large field. This could be a significant source of error for the evapotranspiration and crop yield modeling approaches (Wiegand *et al.*, 1979). "Ground-truth" sampling must adequately account for the *in situ* population variability by inclusion of enough samples to allow for a reasonable estimate of the actual field leaf area index.

#### DESCRIPTION OF RESEARCH UNDERTAKEN

As part of an on-going research program into future satellite sensor development including selection and evaluation of spectral bands, radiometric resolution, frequency of coverage, orbit selection, and other considerations for vegetational applications, we have been collecting hand-held radiometer data from a variety of agricultural crops in a NASA/GSFC-USDA/BARC cooperative research program. Previous research on alfalfa, corn, and soybeans had demonstrated that red and photographic infrared two-band radiometer data were highly correlated with various properties of plant canopies (Tucker *et al.*, 1979a,b,c; Holben *et al.*, 1980). Therefore, we

decided to evaluate the applicability of these data for yield predictions on wheat. A companion paper reports on the use of these data for monitoring total dry matter accumulation (Tucker *et al.*, 1980b).

Previous work with the green leaf or photosynthetically active biomass has suggested that this physiological entity integrated the various biotic and abiotic effects present in plant canopies (Colwell *et al.*, 1977; Tucker *et al.*, 1979a,b). Many conditions which adversely affect plant growth and development result in a reduction in the photosynthetically active biomass. Because the photosynthetically active biomass or green leaf area is one of the basic system variables in primary production, monitoring this system variable throughout the growing season should enable inferences to be made regarding total dry matter accumulation and grain yield. This has been proposed as the leaf area duration (LAD) concept (Colwell *et al.*, 1977; Richardson *et al.*, 1979).

However, the LAD concept needs to be modified in that the photosynthetically active biomass or leaf area is actually the interaction between the green LAI and the chlorophyll concentration. Expressed in other words, the photosynthetically active biomass can be defined as the interaction between inter- and intra-leaf scattering and chlorophyll absorption which occurs predominantly in the green leaves of the plant canopy in question. Thus, we are actually interested in the duration and magnitude of the green leaf area index.

Red and photographic infrared spectral data have been demonstrated by many workers to be highly correlated with the photosynthetically active biomass of several cover types (reviewed in Tucker, 1979). The red spectral data are highly correlated with the *in vivo* chlorophyll concentration whereas the photographic infrared data are highly correlated with the green LAI. Thus, various linear combinations of these two adjacent spectral regions are highly related to the photosynthetically active biomass (Tucker, 1979).

#### EXPERIMENTAL PROCEDURE

Our experiment was conducted in a 1.2-ha soft red winter wheat (*Triticum aestivum* L.) field at the Beltsville Agricultural Research Center, Beltsville, Maryland. The field was plowed, disked, and planted with the cultivar 'Arthur' on 6 October 1977 at a rate of 107.6 kg/ha. A conventional grain drill with 17.8-cm row spacing was used for seeding. Before seeding, the field was limed on the

basis of soil test recommendations and fertilizer was applied at a rate of 33.3 kg N, 53.8 kg P, and 53.8 kg K/ha. The following spring (early March 1978) the crop was topdressed with 20.4 kg N/ha.

Twenty 2- by 3-m plots were selected during the winter dormant period in the wheat field. Subsequently, for each plot four pairs of red (0.65-0.70  $\mu\text{m}$ ) and photographic infrared (0.775-0.825  $\mu\text{m}$ ) spectral radiance measurements were obtained using a hand-held digital radiometer (Pearson *et al.*, 1976) on 21 dates between 21 March 1978 (Julian date 80) and 23 June 1978 (Julian date 174). The intervals between dates varied from one to nine days; however, the average interval was 4.7 days and the median interval was a tie between four and five days (Table 1).

The red and photographic infrared spectral radiance data were used to form the IR/red radiance ratio and the normalized difference (ND) of Rouse *et al.* (1973) and Deering *et al.* (1975) where

$$\text{ND} = (\text{IR} - \text{RED})/(\text{IR} + \text{RED}) \quad (1)$$

The four pairs of the spectral measurements per plot were averaged to account for the spatial variability present in each plot. All spectral data were collected at plus or minus 90 minutes of local solar noon, mea-

sured normal to the ground surface at a height of ~1 m above the plant canopy, and were collected under sunny skies (Table 1).

Throughout the growing season average plant height, percentage cover estimates, and phenological development notes were recorded for the field area (Table 2). The crop matured in late June 1978. On 28 June 1978 (Julian date 179) a 0.9- by 3.0-m swath was cut with a small sickle bar mower from the center of each plot. Total biomass and grain yield were recorded. The sample was thrashed with a small grain thrasher. The entire grain yields were oven dried at 60°C for 72 hours and were subsequently adjusted to 14 percent moisture and expressed in  $\text{g}/\text{m}^2$ .

Grain yield ranged from 220  $\text{g}/\text{m}^2$  (~30 bu/ac) to 410  $\text{g}/\text{m}^2$  (~60 bu/ac). The within-field difference in grain yield between plots occurred regardless of the field level controls described earlier. Within-field grain yield variability was probably a function of subsurface soil micro-characteristics such as soil water, soil type, fertility, etc., for which measurements were beyond the scope of this study. Rather, we chose to account for these effects of within-field grain yield variability by measuring red and photographic infrared spectral radiances throughout the spring portion of the growing season (i.e., red and photographic infrared

TABLE 1. TABULAR LISTING OF THE DAYS WHEN HAND-HELD RADIOMETER DATA WERE COLLECTED FROM THE 20 2 × 3 m WINTER WHEAT PLOTS IN 1978

Sampling Sequence	Julian Date	Time (EST)	Conditions/Comments (Temperature, Sky, Wind, Etc.)
1	80	1130-1215	12°C, clear with no clouds, wind = 16 kmh
2	89	1215-1300	8°C, clear with no clouds, calm, soil damp
3	92	1222-1310	15°C, clear with no clouds, calm
4	95	1220-1245	17°C, a few scattered clouds, wind = ~5-10 kmh
5	97	1225-1247	21°C, a few scattered clouds, calm
6	102	1110-1135	14°C, clear with no clouds, wind = ~5 kmh
7	104	1210-1230	20°C, clear with no clouds, wind = 30-45 kmh
8	112	1338-1415	18°C, scattered clouds, gusty wind = 5-20 kmh
9	118	1230-1310	22°C, clear with no clouds, gusty wind = 5-30 kmh
10	121	1200-1230	16°C, clear with no clouds, wind = 5-10 kmh
11	123	1215-1250	18°C, clear with no clouds, calm
12	131	1145-1210	24°C, a few scattered clouds, wind = ~10 kmh
13	139	1145-1230	20°C, a few scattered clouds, wind = <15 kmh
14	146	1125-1205	19°C, a few scattered clouds, calm
15	152	1130-1200	22°C, clear with no clouds, wind = 5-10 kmh
16	157	1050-1120	22°C, a few scattered clouds, wind = ~10 kmh
17	161	1230-1300	26°C, clear with no clouds, calm
18	165	1030-1125	17°C, a few scattered clouds, wind = 25-40 kmh
19	166	1100-1200	20°C, high faint cirrus, calm
20	170	1030-1100	20°C, a few scattered clouds, wind = <10 kmh
21	174	1100-1130	28°C, clear with no clouds, calm

Mean time between sampling dates = 4.7 days

Range between sampling dates = 1-9 days

Medium time between sampling dates = 4.5 days (tie)

TABLE 2. AGRONOMIC DATA PERTAINING TO AVERAGE PLANT HEIGHTS, ESTIMATED PERCENTAGE CANOPY COVER, AND CROP GROWTH STAGES AT 11 SELECTED DATES FOR THE 20 WINTER WHEAT PLOTS FROM 1978

Calendar Date	Julian Date	Plant Height (cm)	Percentage Cover	Growth Stages	
				Numerical (after Zadoks et al., 1974)	Descriptive
04/24/78	114	35.0	54	34	stem elongation, 4th node detectable
05/01/78	121	45.2	56	35	stem elongation, 5th node detectable
05/11/78	131	70.8	66	44	booting, boots just visible
05/19/78	139	90.8	64	58	inflorescence emerges
05/25/78	145	112.0	68	64	anthesis, half-way
06/01/78	152	112.5	61	73	early milk
06/06/78	157	114.8	63	85	soft dough
06/14/78	165	115.5	64	85	soft dough
06/20/78	171	111.8	51	87	hard dough
06/23/78	174	108.5	51	89	hard dough
06/27/78	178	104.0	51	92	ready for harvest

radiance are highly correlated to the green leaf biomass which is usually highly correlated to yield). We feel that significant within-field yield variability can occur unless the above ground and below ground factors which influence yield are very nearly equal for the field(s) in question. This obviously is not the case for many fields and it was not the case for our winter wheat field.

A regression approach was taken in which the average red radiance, IR radiances, IR/red ratio, and ND were correlated with the grain yield for each of the 21 data collection dates. In addition, the IR/red ratio and the ND as a function of Julian date and growing degree days were integrated for four different time intervals and correlated with grain yield.

#### RESULTS AND DISCUSSION

Examples of the radiance data were plotted against Julian date (Figure 1). The red radiance versus Julian date curve showed the influence of increasing chlorophyll absorption (lower radiance) as a result of increasing green vegetation. A rapid increase in the radiance occurred after Julian date 150 due to chlorosis of the maturing crop (Figure 1a). The photographic infrared radiance versus Julian date curve showed a gradual increase with time to a maximum at ~Julian date 139 followed by a decrease caused by senescence. This resulted from the direct relationship of the photographic infrared radiance to the foliar density of the plant canopy (Figure 1b). The IR/red radiance ratio and the normalized difference both exhibited similar trends with respect to Julian

date (Figures 1c and 1d, respectively). Both spectral variables showed the same five component trends with respect to Julian date: They both increased as the spring portion of the growing season began until ~Julian date 102 where their rate of increase declined; from Julian date ~102 to ~112 both showed rapid rates of increase; from Julian date ~112 to ~123 there was a decrease for both spectral variables; from Julian date ~123 to ~139 there was another increase in both spectral variables; and from Julian date ~139-175 there was the senescence caused decrease in both the IR/red radiance ratio and the normalized difference.

These same trends were observed for the majority of our experimental plots and were an example of a manifestation of transient wheat canopy water stress (Figure 2). The IR/red radiance ratio and the normalized difference both exhibited a decrease in their rate of increase by Julian date ~102. This decrease was ended by a period of rainfall on Julian day 106-107 which resulted in a rapid rate of increase in the IR/red radiance ratio and normalized difference until Julian date ~112 when another period of mild drought stress began and intensified until ~Julian date 123. The later episode of drought stress was ended by a period of week-long rains which prevented any field data collection for the interval of Julian dates 124-130. The plant canopy subsequently recovered from the previous water stress condition and reached maximum values of the IR/red radiance ratio and the normalized difference on Julian date 139 which corresponded to

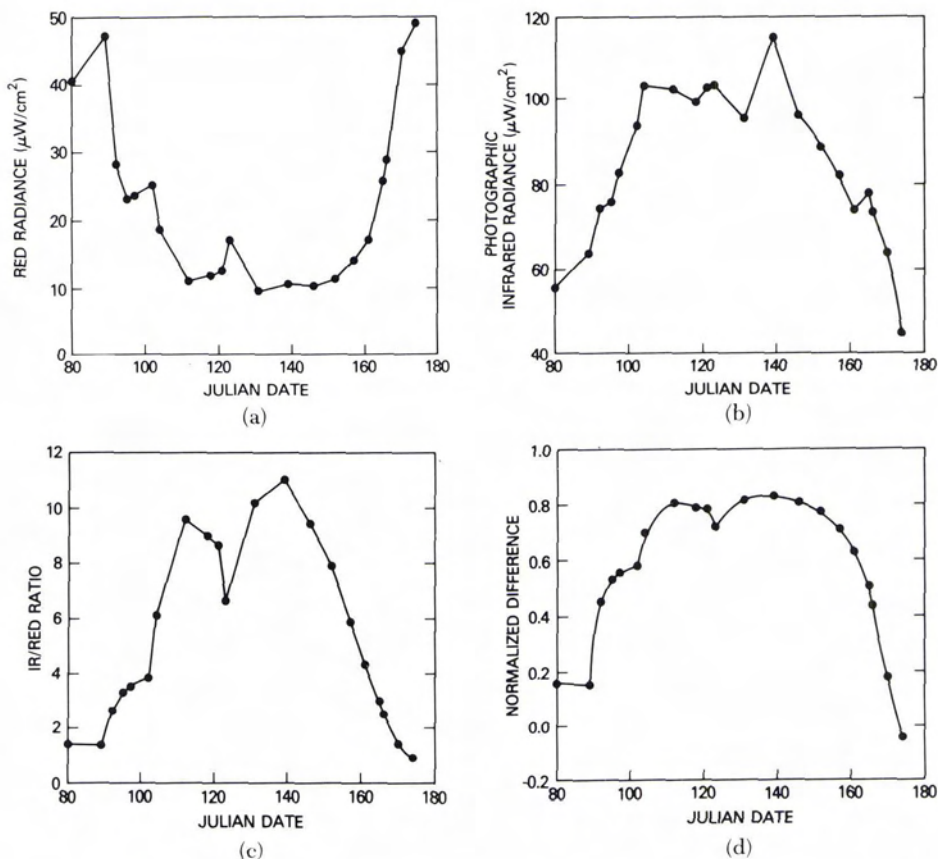


FIG. 1. Red radiance, photographic infrared radiance, IR/red radiance ratio, and the normalized difference plotted against Julian date for one of 20 wheat plots sampled. (a) Red radiance, (b) photographic infrared radiance, (c) IR/red radiance ratio, and (d) normalized difference (ND). Note how the IR/red radiance ratio and the normalized difference effectively compensate for the variability in the radiance data.

full spike emergence (Table 2). From this date on, the progression of wheat canopy senescence resulted in a reduction of the IR/red radiance ratio and the normalized difference (Figure 2).

The spectral manifestation of drought stress was consistent with previous research results (Thompson and Wehmanen, 1979; Tucker, *et al.*, 1980a). Figure 2 also demonstrated the dynamic nature of our wheat canopy and how rapidly it responded to and recovered from water stress conditions. We interpreted the mechanism for this spectral manifestation of plant canopy water stress to be largely due to a reduction in the leaf chlorophyll density and/or canopy geometry changes. This followed from Figure 1a where there were decreases in red absorption (i.e., increases in red radiance) for Julian dates 102 and 123 which corresponded to the

episodes of water stress. The photographic infrared radiance, by contrast, did not show the same degree of effect which was attributed to the episodes of water stress (Figure 1b). This implied that the LAI remained fairly constant while the leaf chlorophyll density was temporarily reduced, either through photooxidation, enzymatic, or some other reducing mechanism (Tucker *et al.*, 1973; Tucker *et al.*, 1980a).

The next phase of the analysis regressed each of the four spectral variables against the final grain yield for each of the 21 data collection dates. Our principal attention was focussed on the IR/red radiance ratio and the normalized difference as these linear combinations adjust for sun elevation induced irradiational variability (Figure 3). We observed lower correlations for the first four dates, higher correlations for dates 5 and 6,

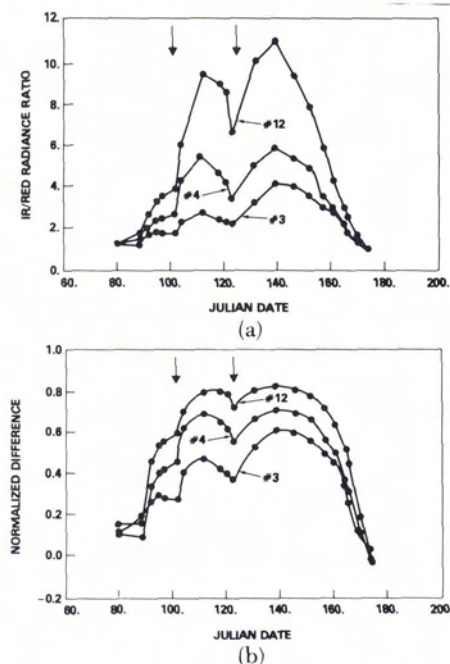


FIG. 2. The IR/red radiance ratio (a) and the normalized difference (b) from three 2- by 3-m plots plotted against Julian date. The vertical arrows represent episodes of rainfall. Note the response of the two spectral variables to the occurrence of precipitation which ended periods of water stress. The numbers 3, 4, and 12 identify individual experimental plots. Rainfall records were available from a weather station 1 km from our experimental field.

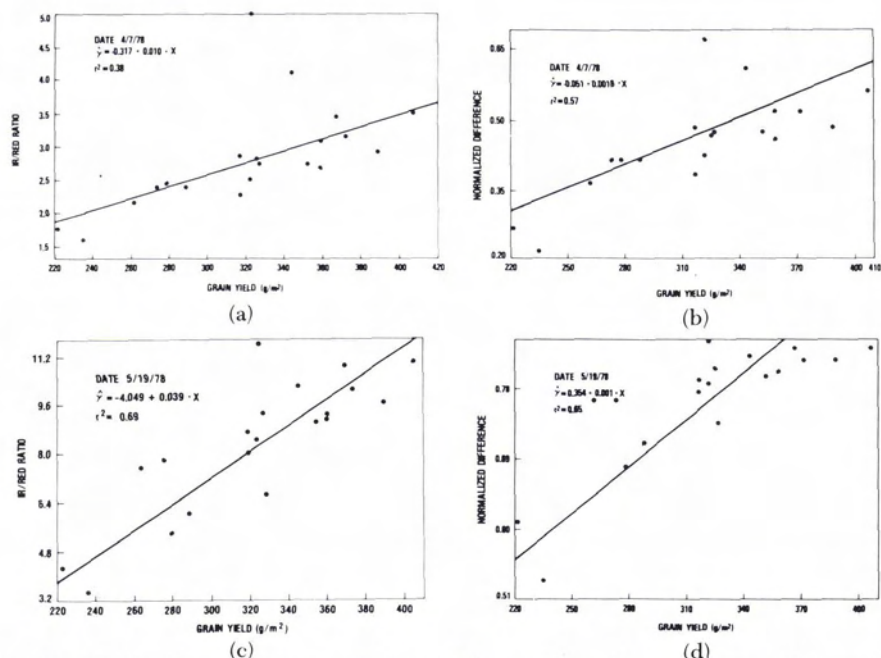


FIG. 3. The IR/red radiance ratio and normalized difference plotted against grain yield for two sampling dates.

and a marked decrease in correlation with grain yield for date 7 which was attributed to very windy conditions (Tables 1 and 3). Sampling dates 8, 9, and 10 were all highly correlated to grain yield, there was a slight decrease for date 11, followed by high correlations for sampling date 13, after which the correlations decreased as senescence progressed (Figure 4). Windy conditions were also present for sampling date 18 (Julian date 165). Data from this date were found to explain 6 percent and 4 percent less grain yield variability than data taken one day later under calm conditions for the IR/red radiance ratio and normalized difference, respectively (Tables 1 and 3; Figure 4).

We observed a 40-day period (from Julian date 112-152) during which our spectral data were more significantly correlated to the final grain yield than earlier or later (Figure 4; Table 3). However, the regression relationships were not constant during this period, suggesting that a regional application of these relationships was doubtful (Table 4). An alternative to this was attempted in the form of integrating the spectral data in terms of Julian date or accumulated temperature units (growing degree days or equivalent). This was a remote sensing application of the leaf area duration concept.

The IR/red radiance ratio and the normalized difference were integrated for four periods during the growing season: Julian dates

TABLE 3. CORRELATION COEFFICIENTS FOR THE FOUR RADIANCE VARIABLES AND FINAL GRAIN YIELD FOR EACH OF THE 21 DAYS WHERE SPECTRAL DATA WERE COLLECTED FROM 20 2 × 3 PLOTS IN 1978. REFER ALSO TO FIGURES 3 AND 4.

Sampling Sequence	Julian Date	Red Radiance	Ir Radiance	Ir/Red Radiance Ratio	Normalized Difference
1	80	0.14	0.51*	0.27	0.27
2	89	-0.33	0.48*	0.41	0.43
3	92	-0.22	0.42	0.31	0.30
4	95	-0.30	0.43	0.40	0.42
5	97	-0.71**	0.78**	0.62**	0.75**
6	102	-0.71**	0.80**	0.61**	0.75**
7	104	-0.51*	0.59**	0.55*	0.57**
8	112	-0.75**	0.74**	0.69**	0.78**
9	118	-0.82**	0.66**	0.73**	0.82**
10	121	-0.82**	0.54*	0.76**	0.82**
11	123	-0.78**	0.64**	0.68**	0.79**
12	131	-0.76**	0.78**	0.75**	0.78**
13	139	-0.78**	0.83**	0.83**	0.81**
14	146	-0.73**	0.76**	0.77**	0.76**
15	152	-0.78**	0.69**	0.78**	0.78**
16	157	-0.73**	0.61**	0.71**	0.73**
17	161	-0.55**	0.68**	0.66**	0.66**
18	165	-0.51*	0.49*	0.56**	0.55**
19	166	-0.57**	0.43	0.61**	0.58**
20	170	0.19	0.51*	0.32	0.30
21	174	0.46*	-0.14	-0.48*	-0.42

\* Indicates significance at the 0.05 level of probability

\*\* Indicates significance at the 0.01 level of probability

80-112; 112-152; 152-174; and 80-174. We observed that the plateau portion (Julian dates 112-152) of the growth curves, corresponding to the maximum green leaf biomass present, were the most highly correlated with final yield (Figure 5). The normalized difference spectral data from this period explained 66 percent of the within-field variability in final grain yield while the normalized difference spectral data from the entire growing season (i.e., Julian dates 80-174) explained 64 percent of the same grain yield variability (Figures 5 and 6). Spectral data alone thus explained approximately two-thirds of the variability in within-field grain yield. This could not be explained by meteorological models as the micro-climatic effects were largely identical for our 1.2-ha field. Soil micro-characteristics described earlier would probably explain the remaining one-third of the yield variability. The earlier integration period of Julian date 80-112 only explained 48 percent of the variability in final grain yield while the integration period of Julian date 152-174 only explained 45 percent of the variability in final grain yield (Figure 5). Any successful applications of these relationships for regional remote sensing prediction of winter wheat grain yield must be able to account for

within region differences in winter wheat crop phenology. From Table 4 we showed that the regression derived equation coefficients varied for the 40-day period (Julian dates 112-152) where highly significant correlations between the spectral data and final grain yield were reported (Tables 3 and 4). Thus, crop phenology differences within a given region would preclude the effective use of one or two satellite images obtained during this five- to six-week period. Either accurate crop calendar information must be available or the leaf area duration technique must be employed.

Crop calendar information is frequently lacking in extra-country situations. A possible remotely sensed substitute for this could be the combination of spectral data and accumulated temperature units (Figure 7). This follows from the basic relationship of temperature to biological activity. When combined with red and photographic infrared spectral data, representing the plant canopy vigor or potential for growth, this may have between-region and/or between-year comparison utility.

In the event that a combination of spectral and accumulated temperature unit data would be unsatisfactory, frequent satellite coverage would be required to apply the leaf

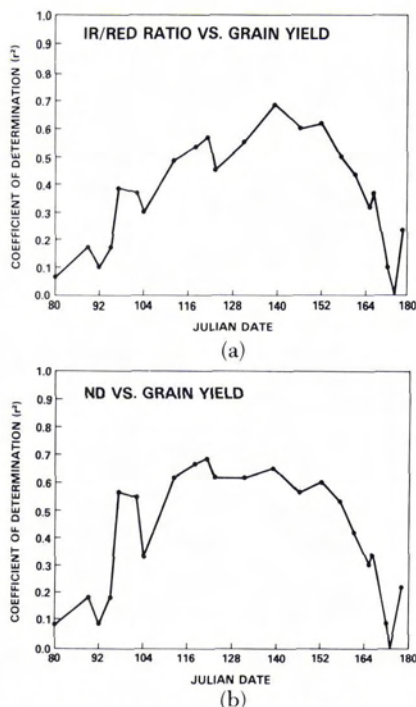


FIG. 4. Coefficients of determination resulting from regressing the (a) IR/red radiance ratio or (b) normalized difference against grain yield for each of the 21 data collection dates. The  $r^2$  values presented in Figure 3 are plotted against Julian date along with the respective  $r^2$  values for the other 19 dates. Note how the normalized difference was more highly correlated with final grain yield than was the IR/red radiance ratio earlier in the growing season. The 7th and 18th sampling dates show the effects of strong wind upon the spectral data (see also Tables 1 and 3).

area duration concept for growing season integration of spectral data. As shown in Figure 2, frequent satellite coverage is needed to record the rapid onset of plant

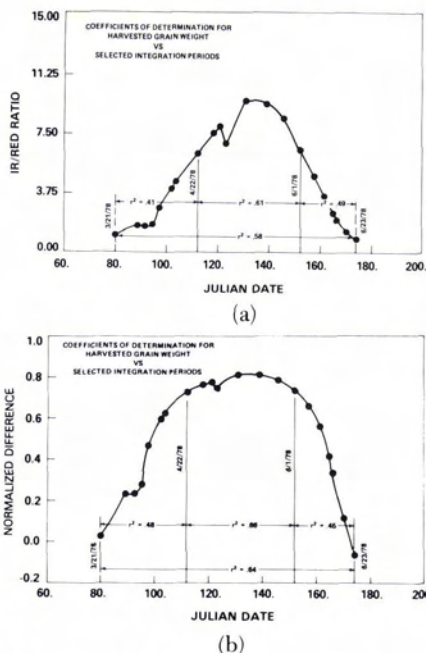


FIG. 5. The  $r^2$  values resulting from the (a) IR/red radiance ratio—Julian date and (b) normalized difference—Julian date integrations for four different time periods: Julian dates 80-112; 112-152; 152-174; and 80-174. (Refer also to Figure 6.)

canopy stress conditions. It is easy to visualize the situation in Figure 2 if there were only four, five, or six data points instead of the 21 we collected. Obviously, entire stress periods might not be detected if only a few observations were available. For yield considerations, the occurrence of the stress condition is of paramount importance. If a period of water stress occurs during heading or during the grain filling period, the reduction of the grain yield is much greater than if this

TABLE 4. REGRESSION DERIVED ESTIMATES FOR  $\beta_0$  AND  $\beta_1$  FOR JULIAN DATES 112-152 USING THE IR/RED RADIANCE RATIO AND THE NORMALIZED DIFFERENCE TO PREDICT THE FINAL GRAIN YIELD. THE EQUATION USED WAS OF THE FORM GRAIN YIELD =  $\beta_0 + \beta_1$  (SPECTRAL VARIABLE)

Sampling Period	Julian date	IR/Red Radiance Ratio			Normalized Difference		
		$\beta_0$	$\beta_1$	$r^2$	$\beta_0$	$\beta_1$	$r^2$
8	112	225.6	14.7	0.48	69.1	365.0	0.61
9	118	230.0	15.3	0.53	85.6	350.3	0.67
10	121	224.4	15.0	0.57	96.6	327.0	0.68
11	123	231.5	17.2	0.46	116.8	321.1	0.62
12	131	207.7	15.0	0.56	15.8	413.7	0.61
13	139	173.1	17.8	0.69	-70.3	511.7	0.65
14	146	170.8	21.5	0.59	-26.8	475.7	0.57
15	152	148.4	29.0	0.61	-51.2	534.0	0.60



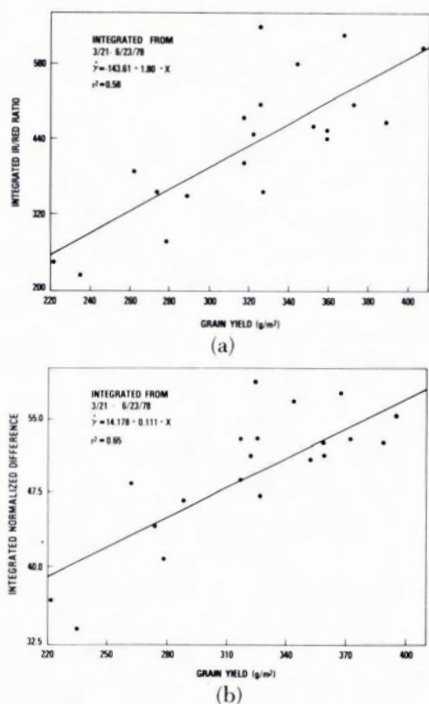


FIG. 6. The relationship between the (a) integrated IR/red radiance ratio and the (b) integrated normalized difference and final grain yield for the spring portion of the growing season (refer also to Figure 5).

same stress condition occurs at some other time.

Spectral data are capable of providing large-area information highly related to crop condition or vigor. Whether these data are used in conjunction with other remotely sensed information, by simulation modelers,

or by themselves, it is apparent that remotely sensed red and photographic infrared spectral data can supply valuable crop condition information.

#### CONCLUSIONS

- Frequently collected spectral data were shown to be highly related to crop condition. Two periods of water stress were readily apparent.
- A 40-day period existed during which the spectral data explained at least 60 percent of the variability in within-field grain yield on a per date basis.
- Spectral data explained two-thirds of the variability in within-field final grain yield. This could not be explained using meteorological models as the micro-climate conditions were very similar for our experimental wheat field. Subsurface soil micro-characteristic differences were thought to have resulted in the range of grain yields reported herein.
- A substantial amount of within-field grain yield variability was found to exist. Care must be taken in field level sampling to account for this variability.
- Windy conditions were found to degrade the relationship(s) between the spectral data and grain yield.
- Large-scale extra-country application of our findings would require a spectral crop calendar. We propose a possible spectral-accumulated temperature units crop calendar. If this is not feasible, we suggest frequent satellite observations and application of the leaf area duration concept.
- The combination of spectra data and other environmental or agronomic data will improve the predictive utility of yield forecasting. While spectra data are useful by themselves, they are more useful in combination with other types of data.

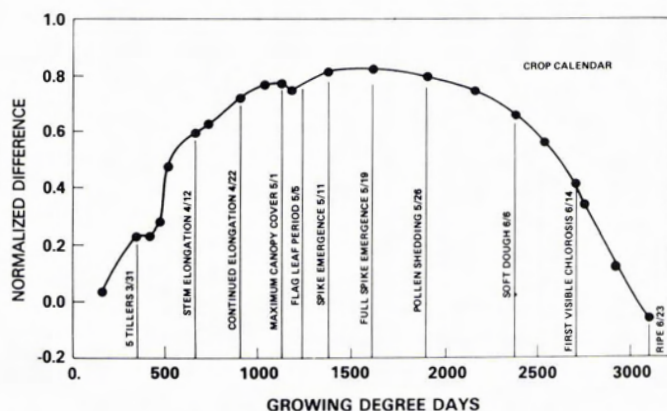


FIG. 7. A possible spectral crop calendar using the normalized difference and accumulated temperature units (i.e., growing degree days). Growing degree days were calculated using a 40°F base temperature.

## ACKNOWLEDGMENTS

We thank Paul Pinter, Jr., Ray Jackson, John Colwell, and Wayne Willis for encouragement and suggestions on the manuscript. We thank the following people for help in the collection of data in the field: Chris Justice, Dan Kimes, Donna Strahan, Diana Crowley, Maryann Karinch, Charley Walthall, Josette Pastor, Jelle Hielkema, Steve Bogash, Don Friedman, Bill Jones, and Bill Wigton. We thank Freeman Smith for the loan of the instrument.

## REFERENCES

- Colwell, J. E., D. P. Rice, and R. F. Nalepka, 1977. Wheat yield forecasts using Landsat data. In *Proc. of the 11th International Symposium on Remote Sensing of Environment*, Univ. of Michigan, Ann Arbor, pp. 1245-1254.
- Deering, D. W., J. W. Rouse, R. H. Hass, and J. A. Schell, 1975. Measuring forage production of grazing units from Landsat MSS data. *Proc. of the 10th International Symposium on Remote Sensing of Environment*, pp. 1169-1178.
- EarthSat Corp., 1976. *EarthSat Spring wheat yield system test*. Final Report, Washington, DC.
- Harlan, J. C., and S. Liu, 1975. *A one year, one site Landsat Study for determination of unharvested winter wheat acreage*. Tech Report RSC-66, Remote Sensing Center, Texas A&M Univ., College Station.
- Hammond, A. L., 1975. Crop forecasting from space: Toward a global food watch. *Science*, 188, pp. 434-436.
- Heilman, J. L., E. T. Kanesmasu, J. O. Bagley, and V. P. Rasmussen, 1977. Evaluating soil moisture and yield of winter wheat in the Great Plains using Landsat data. *Remote Sensing of Environment*, 6, pp. 315-326.
- Holben, B. N., C. J. Tucker, and C. J. Fan, 1980. Spectral assessment of soybean leaf area and leaf biomass. *Photogram. Engr. and Remote Sensing*, 46(5), pp. 651-656.
- Idso, S. B., R. D. Jackson, and R. J. Reginato, 1977a. Remote sensing of crop yield. *Science*, 196, pp. 19-25.
- , 1976b. Albedo measurements as a technique for the remote sensing of crop yields. *Nature*, 266, pp. 625-628.
- Kanemasu, E. T., J. L. Heilman, J. O. Bagley, and W. L. Powers, 1977. Using Landsat to estimate evapotranspiration of winter wheat. *Environmental Management*, 2(6), pp. 515-520.
- LACIE, 1978. *Briefing materials for technical presentations*. The LACIE Symposium, NASA/JSC, Vol. B, Houston, Texas.
- MacDonald, R. B., and F. G. Hall, 1977. LACIE: A look to the future. In *Proc. of the 11th International Symposium on Remote Sensing of Environment*. Univ. of Michigan, Ann Arbor, pp. 429-465.
- Morain, S. A., and D. L. Williams, 1975. Wheat production estimates using satellite images. *Agron. J.*, 67, pp. 361-364.
- Pearson, R. L., L. D. Miller, and C. J. Tucker, 1976. Hand-held radiometer to estimate gramineous biomass. *Appl. Opt.* 15(2), pp. 416-418.
- Richardson, A. J., C. L. Wiegand, J. F. Arken, P. R. Nixon, and A. H. Gerberman, 1979. Spectral indicators of sorghum development and their implications for growth modeling. To be submitted to *Photogram. Engr. and Remote Sensing*.
- Rouse, J. W., R. H. Haas, J. A. Schell, and D. W. Deering, 1973. Monitoring vegetation systems in the Great Plains with ERTS. *Third Symposium on Significant Results Obtained with ERTS-1*. NASA SP-351, pp. 309-317.
- Thompson, D. R., and O. A. Wehmanen, 1979. Using Landsat digital data to detect moisture stress. *Photogram. Engr. and Remote Sensing*, 45(2), pp. 201-207.
- Tucker, C. J., 1979. Red and photographic infrared linear combinations for monitoring vegetations. *Remote Sensing of Environment*, 8(2), pp. 127-150.
- Tucker, C. J., J. H. Elgin, and J. E. McMurtrey, 1979a. Temporal spectral measurements of corn and soybean crops. *Photogram. Engr. and Remote Sensing*, 45(5), pp. 600-608.
- Tucker, C. J., J. H. Elgin, J. E. McMurtrey, and C. J. Fan, 1979b. Monitoring corn and soybean crop development with hand-held radiometer spectral data. *Remote Sensing of Environment*, 8(3), pp. 237-248.
- Tucker, C. J., J. H. Elgin, and J. E. McMurtrey, 1980a. Relationship of red and photographic infrared spectral radiances to alfalfa biomass, forage water content, percentage canopy cover, and severity of drought stress. *International Journal of Remote Sensing* (in press).
- Tucker, C. J., B. N. Holben, J. H. Elgin, and J. E. McMurtrey, 1980b. *Remote sensing of winter wheat total dry matter accumulation*. NASA/GSFC Technical Memorandum 80631.
- Tucker, C. J., L. D. Miller, and R. L. Pearson, 1973. Measurement of the combined effect of green biomass, chlorophyll, and leaf water on canopy spectrorreflectance of the short-grass prairie. *Proc. of the 2nd Annual Remote Sensing of Earth Resources Conf.*, Space Inst. of Tenn. Univ., pp. 601-627.
- Wiegand, C. L., A. J. Richardson, and E. T. Kanemasu, 1979. Leaf area index estimates for wheat from Landsat and their implications for evapotranspiration and crop modeling. *Agron. J.*, 71, pp. 336-342.
- Zadoks, J. C., T. T. Chang, and C. F. Konzak, 1974. A decimal code for the growth stages of cereals. *Weed Research*, 14, pp. 415-421.

(Received 26 July 1979; revised and accepted 17 November 1979)